

# INTERBAND OPTICAL TRANSITIONS IN THE REGION OF EXCITON RESONANCES IN $\text{In}_{0.3}\text{Ga}_{0.7}\text{As}/\text{GaAs}$ QUANTUM WELLS

N. Syrbu<sup>1</sup>, A. Dorogan<sup>1</sup>, V. Dorogan<sup>1</sup>, T. Vieru<sup>1</sup>, V. Ursaki<sup>2</sup>, and V. Zalamai<sup>2</sup>

<sup>1</sup>*Technical University of Moldova, Stefan cel Mare Avenue 168, Chisinau, MD-2004 Republic of Moldova*

<sup>2</sup>*Institute of Applied Physics of the Academy of Sciences of Moldova, Academiei str. 5, Chisinau, MD-2028 Republic of Moldova*

(Received 2 October 2012)

## Abstract

Reflectance spectra of quantum wells (QWs) with 8-nm-thick  $\text{In}_{0.3}\text{Ga}_{0.7}\text{As}$  layers with a 9-nm-thick GaAs barrier layer up and a 100-nm-thick barrier layer down were investigated in the spectral range of 0.5–1.6 eV in S- and P- polarizations at an incidence angle close to the normal ( $7^\circ$ ) as well as at a Brewster angle ( $76^\circ$ ). Narrow lines at 0.9021; 1.0161; 1.1302; 1.1973; and 1.2766 eV were observed in the reflectance and absorption spectra, which are due to hh, lh1-e1(1s), hh1, lh1-e2(1s), hh2, lh2-e2(1s), and hh3, lh3-e3(1s) transitions, as well as features due to quantum dots (QDs) formed at the interface of nanolayers and the buffer. The contours of reflectance and absorption spectra are calculated with a single-oscillator, and many-oscillator models. The oscillator strength and the damping parameter are estimated for the optical transitions in QWs and QDs. The radiative life time of the exciton in a QW and a QD was found to be  $\tau_0 = (2\Gamma_0)^{-1} \approx 2 \times 10^{-12}$  s.

## 1. Introduction

The optical properties of heterostructures with  $\text{In}_{0.3}\text{Ga}_{0.7}\text{As}/\text{GaAs}$  quantum wells (QWs) are determined mainly by the high efficiency of interaction of the quasi-two-dimensional exciton subsystem with the light. The investigation of semiconductor nano-heterostructures is important from the point of view of both the determination of fundamental properties of excited QW and QD states and the development of a new generation of optoelectronic and microelectronic devices [1-3]. Nowadays, injection lasers based on quantum dots QDs have been demonstrated with an ultra-high thermal stability of the threshold current  $J_{\text{th}}$ , a low value of the  $J_{\text{th}}$  [4–6], and generating in a continuum wave mode at room temperature with a high output power above 3 W [7-12]. One of the advantages of using structures with QDs is the possibility to extend the optical diapason of the emission as compared to structures with QWs. Thus, structures with  $\text{In}(\text{Ga})\text{As}/(\text{Al})\text{GaAs}$  QDs allow one to obtain emission in the range of 1–1.6  $\mu\text{m}$  [8–12]. In particular, the structures with QDs are promising for the development of devices generating at wavelength of 1.3  $\mu\text{m}$  [9–11].

In this study, we investigate the interband optical transitions in the region of exciton resonances in  $\text{In}_{0.3}\text{Ga}_{0.7}\text{As}/\text{GaAs}$  QWs. The contours of reflectance and absorption spectra related to the ground exciton polariton states in QWs are calculated.

## 2. Experimental

The optical reflectance and transmission spectra were measured with MDR-2 and JASCO-670 at temperatures of 10 and 300 K in s- and p- polarizations at different incidence angles of the light at the surface of the hetero-nanostructure. When necessary, the fine structure of spectra was measured with a high-aperture (1:2) double-grating high-resolution SDL-1 spectrometer. An InGaAsP photodiode was used as photodetector. The samples were mounted on the cold station of a LTS-22-C-330 cryogenic system for cooling. The back-side surface of the structure was polished to a mirror-state for the investigation of transmittance spectra  $T(\omega) = |t(\omega)|^2$ .

## 3. Results and discussion

### 3.1 Reflectance and transmission spectra of $\text{In}_{0.3}\text{Ga}_{0.7}\text{As}/\text{GaAs}$ heterostructures with QWs

The transitions induced by the light with photon energies  $\hbar\omega > E_g$  between different subbands of the V-band to subbands of the C-band produced by dimensional quantization in QWs can generate a whole family of electronic transitions, i.e., interband reflection, absorption and luminescence bands [13-15]. The reflection  $R(\omega) = |r(\omega)|^2$  and transmission  $T(\omega) = |t(\omega)|^2$ , as well as the luminescence, are versatile techniques for investigating QWs in heterostructures. For the determination of absorption  $A(\omega)$  in structures with QWs, it is necessary to measure the reflection  $R$  and transmission  $T$

$$A(\omega) = 1 - R(\omega) - T(\omega) \quad (1)$$

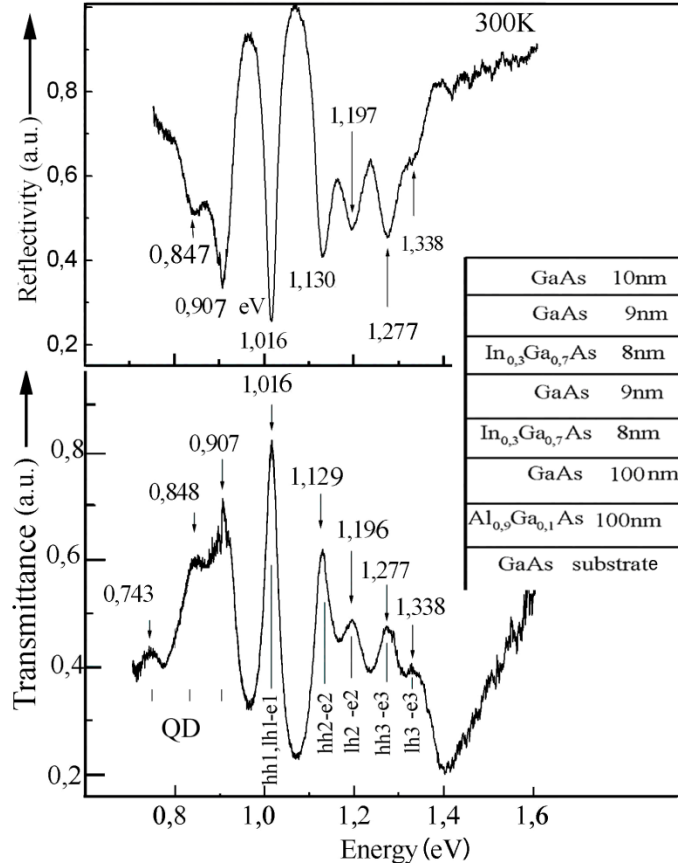
The nonideality of the structure influences the optical reflection and absorption spectra, leading to inhomogeneous broadening of the resonance frequency of excitons in heterostructures. The inhomogeneity can lead to a smooth dependence of  $\omega_0$  upon the coordinate in the plane of the QW, or in the volume of the super-lattice, which results in the broadening of absorption and reflection lines.

From the experimental point of view, the narrow absorption and reflection lines indicate on the high quality of the QW structure. The simplest way to take into account the inhomogeneous broadening when calculating the reflection coefficient is to substitute in the respective formula the non-radiative damping  $\Gamma$  by the effective non-radiative damping  $\Gamma_{\text{eff}} = \Gamma + \Gamma_0$ , where  $\Gamma_0$  is the broadening parameter. Figure 1 shows a structure consisting of two  $\text{In}_{0.3}\text{Ga}_{0.7}\text{As}$  QW layers with a thickness of 8 nm separated by GaAs barrier layers with a thickness of 9 nm. The reflections spectra shown in Fig. 1 were measured at an angle of incidence of the light of  $7^\circ$ , while absorption spectra were measured at normal incidence of the light on the surface of the  $\text{In}_{0.3}\text{Ga}_{0.7}\text{As}/\text{GaAs}$  QW heterojunction. Since the spectra were measured with a high resolution spectrometer, and the maxima in the absorption spectra as well as the minima in the reflection spectra have a FWHM around 2 – meV, one can conclude that the energies of the minima in the reflection spectra coincide with the energies of the maxima in the absorption spectra.

The reflection spectra from a  $\text{In}_{0.3}\text{Ga}_{0.7}\text{As}/\text{GaAs}$  structure with QWs measured at 300 K at incidence angles of  $7^\circ$  and  $76^\circ$  (the Brewster angle) in S-S (A) and P-P (B) polarizations of the light are shown in Fig. 2. The path of the light rays is shown in insets *a* and *b*. Reflection minima b1-b6 are observed in the S-S polarization at an angle of incidence of  $7^\circ$ , these minima being highly broadened at an Brewster angle of incidence.

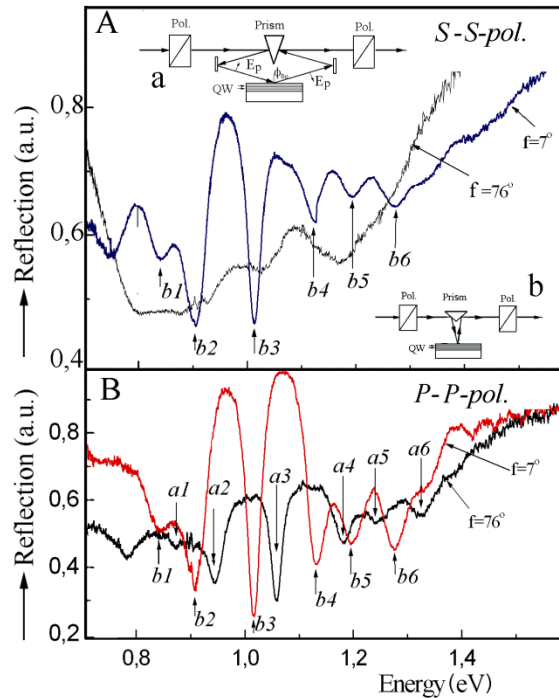
The same b1-b6 minima are observed in the reflection spectra measured in P-P polarization at the angle of incidence of  $7^\circ$ . The minima in the reflection spectra are observed at energies

a1-a6 at a Brewster angle incidence of  $76^\circ$ ; that is, they are shifted. The shift is nearly the same for all the minima. The peak-to-peak amplitude of the reflection spectra is also by a factor of two lower in this polarization. The geometry of the reflection is shown in Fig. 2b. A plane monochromatic wave  $E(r,t) = E_0 \exp(-i\omega t + ikr)$  is incident on a  $\text{In}_{0.3}\text{Ga}_{0.7}\text{As}$  QW placed between two identical GaAs barriers with a real dielectric permittivity  $\epsilon_b$ . The wave vector of the light, related to the frequency  $\omega$  according to the relation  $k = (\omega/c)\sqrt{\epsilon_b}$  (where  $c$  is the speed of the light in vacuum), is also real.



**Fig. 1.** Reflection and absorption spectra of  $\text{In}_{0.3}\text{Ga}_{0.7}\text{As}/\text{GaAs}$  heterojunctions. The structure consisting of two  $\text{In}_{0.3}\text{Ga}_{0.7}\text{As}$  QW layers with a thickness of 8 nm separated by GaAs barrier layers with a thickness of 9 nm is shown in the inset.

The amplitude of the light wave  $E_0$  lies in the plane of the interfaces  $(x,y)$  at a normal incidence of the light, when the wave vector is parallel to the main structure axis  $z$ . Since the system has an axial symmetry with reference to the  $z$ -axis, the electrical vectors of the incident, reflected and transmitted light waves are parallel to each other. Therefore, one can use the scalar amplitudes  $E_0$ ,  $E_r$  and  $E_t$  instead of vector ones. The amplitude coefficients of reflection and transmission of the light are  $r=E_r/E_0$ ,  $t=E_t/E_0$ , respectively. When there is no energy dissipation inside the QW, the energy conservation law imposes the following restriction to these coefficients:  $|r|^2+|t|^2=1$ . The percentage of the absorbed energy inside the QW structure is  $1-|r|^2+|t|^2$ .



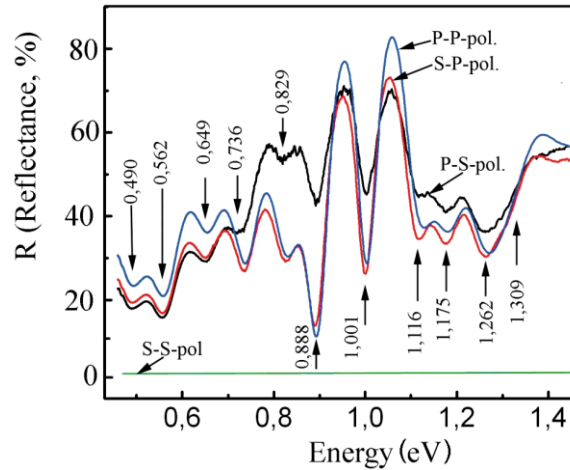
**Fig. 2.** Reflection spectra of an  $\text{In}_{0.3}\text{Ga}_{0.7}\text{As}/\text{GaAs}$  structure with QWs measured at 300 K at angles of incidence of  $7^\circ$  and  $76^\circ$  (the Brewster angle) in S-S (A) and P-P (B) polarization of the light. The path of the light rays is shown in insets (a) and (b).

Figure 3 presents the reflection spectra of a QW structure at different polarizations of the incident and the reflected light waves. No features are observed in the S-S light polarization, while intense bands are observed at 0.9 eV and 1.0 eV in P-P and S-P polarizations.

The reflection, absorption and transmission of an electromagnetic wave which interacts with discrete levels of electron system in a QW in the frequency range corresponding to interband transitions have been investigated in different quantum structures [17, 18]. The results of these investigations are valid for narrow QWs where the following inequality is satisfied

$$Kd \ll 1, \quad (2)$$

where  $d$  is the width of the QW,  $K$  is the module of the wave vector  $\mathbf{k}$  of the light wave. For wide QWs, the parameter  $Kd$  can be  $\approx 1$ . For a heterolaser on the basis of GaAs with a QW with the width of  $500 \text{ \AA}$ , generating at the wavelength of  $0.8 \text{ \mu m}$ , the parameter  $Kd$  is 1.5. For the determination of the electromagnetic field in QWs for which the inequality  $d \gg a_0$  ( $a_0$  is the lattice parameter) is satisfied, one can use the Maxwell equations for a continuous medium [17-19]. This approach allows one to take into account the difference of the refraction coefficients of the barrier and the well. The spatial dispersion of the electromagnetic wave is taken into account in these structures, since its amplitude changes significantly across the well width. The theory which takes into account the spatial dispersion of the electromagnetic wave passing through a QW is described elsewhere [17-19]. An excited level (i.e., an interband transition) has been considered, and refraction coefficients of barriers and QWs for both the monochromatic [18] and the pulsed [19] excitations have been introduced in addition to the spatial dispersion.



**Fig. 3.** Reflection spectra measured at different polarizations of the incident and the reflected light waves.

For the structure considered in this paper, the optical characteristics of the QW and the barrier (the coefficients of refraction and extinction, as well as the real and imaginary parts of the dielectric constant) were calculated from the reflection coefficient by means of the Kramers-Kronig relations. The spectral dependence of the refraction coefficient for different light wave polarizations is shown in Fig. 4. The obtained results suggest that the highest value of the real part of the refraction coefficient is observed in the P-P polarization at the resonance energy of 1.085 eV.

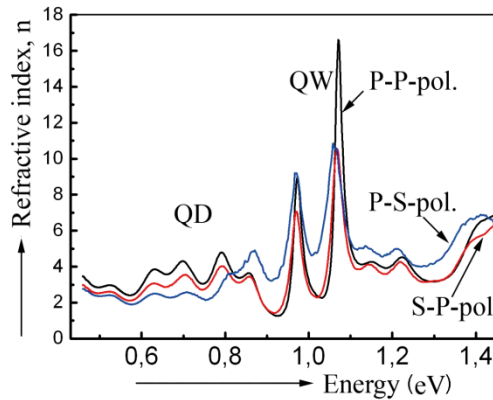


**Fig. 4.** The spectral dependence of the refraction coefficient for different light wave polarizations calculated from the reflection spectra by means of the Kramers-Kronig relations.

Figure 5 presents the spectral dependences of the refractive index  $n$ , the extinction coefficient  $k$ , the real  $\epsilon_1$  and the imaginary  $\epsilon_2$  parts of the dielectric constant for S-P and P-P light wave polarization calculated from the reflection spectra by means of the Kramers-Kronig relation.  $\epsilon_2$  reaches a value near 270 at the energy of 1.085 eV in the P-P light wave polarization, which suggests that the highest absorption is observed at the resonance value of e1-hh1(1s) transitions.

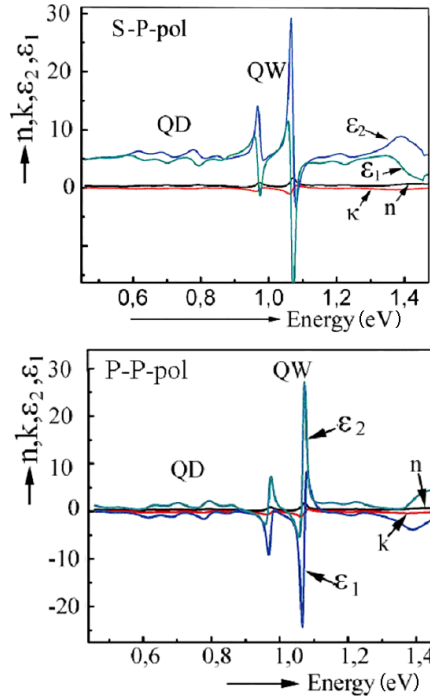


**Fig. 5.** Spectral dependence of the refractive coefficient  $n$ , the exciton coefficient  $k$ , the real  $\epsilon_1$  and the imaginary parts of the dielectric constant for the S-P and P-P light wave polarizations calculated from the reflection spectra by means of Kramers-Kronig relations.

### 3.2 The influence of temperature on the absorption spectra of $\text{In}_{0.3}\text{Ga}_{0.7}\text{As}/\text{GaAs}$ heterojunctions.

The knowledge of semiconductor band structure parameters, particularly the effective mass of carriers, as well as the dependence of these parameters on the composition of layers and temperature is necessary for the determination of parameters of QW structures. The valence band of III-V compounds is four-fold degenerated at  $k=0$ . The application of an axial deformation leads to the appearance of two maxima of the valence band with a small energy separation (the heavy and the light holes). The different maxima (minima) shift to a different degree with the application of an axial deformation in an arbitrary direction. These extremums shift to a higher degree with the temperature change. It is difficult to determine the temperature coefficient of the heavy and light holes valence bands shift. These difficulties are partially overcome in bulk semiconductors by investigating the exciton absorption spectra and the interband magneto-optic effect. For the determination of the temperature coefficient of the heavy and light holes valence bands in  $\text{In}_{0.3}\text{Ga}_{0.7}\text{As}/\text{GaAs}$  heterostructures, we measured the transmission spectra of QW structures at temperatures of 3 and 300 K (Fig. 6).

The digital values on Fig. 6 indicate energy position of the observed transitions in the investigate QW structure. The temperature coefficients of the quantized energy levels as well as the electron and hole bands responsible for these transitions were estimated from these data. The results presented in the table show that the light holes valence bands have a large value of the temperature coefficient, for which  $\beta=\Delta E/\Delta T$  varies in the limits of  $(5.7-7.9)\times 10^{-5}$  eV/K. The temperature coefficient of the heavy holes valence bands varies in the limits of  $(4.4-5.0)\times 10^{-5}$  eV/K. The splitting of the 1S states of light and heavy holes ( $\Delta E_1=\text{lh1-hh1}$ ) at 300 K is 1.7 meV, while it is 3.7 meV at 30 K. The splitting of the  $\Delta E_{12}=\text{lh2-hh2}$  is 4.3 meV

and 10.1 meV at 300 and 30 K, respectively. The same value of splitting is observed for the  $\Delta E_2=lh2-hh2$  interval at both temperatures. The splitting of the  $\Delta E_{33}=lh3-hh3$  transitions is larger: 7.6 and 16.6 meV at 300 and 30 K, respectively (Fig. 7).

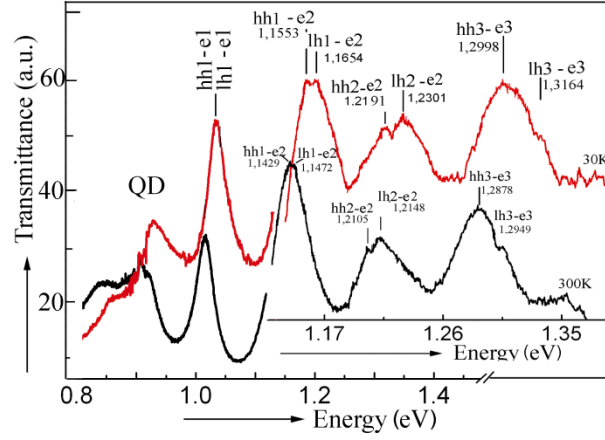


**Fig. 6.** Transmission spectra of an  $In_{0.3}Ga_{0.7}As/GaAs$  QW structure measured at 30 and 300 K, and the energy of electronic transitions in QWs. The high-energy part of the spectrum is presented in a larger scale for the sake of clarity.

**Table.** Energy of electronic transitions in QWs of a  $In_{0.3}Ga_{0.7}As/GaAs$  structure

Transition (1s)	$E_i$ (300K) eV	$E_i$ (30K) eV	$\Delta E = E_i^{30K} - E_i^{300K}$	$B = \Delta E_i / \Delta T$ eV/K
lh1 - e1	1.0249	1.0405	0.0156	$5.8 \times 10^{-5}$
hh1 - e1	1.0232	1.0368	0.0136	$5.0 \times 10^{-5}$
$\Delta E_1 = lh1 - hh1$	1.7 meV	3.7 meV		
lh1-e2	1.1472	1.1654	0.0182	$6.7 \times 10^{-5}$
hh1-e2	1.1429	1.1553	0.0124	$4.6 \times 10^{-5}$
$\Delta E_{12} = lh1 - hh1$	4.3 meV	10.1 meV		
lh2-e2	1.2148	1.2301	1.0153	$5.7 \times 10^{-5}$
hh2-e2	1.2105	1.2191	0.0086	$3.2 \times 10^{-5}$
$\Delta E_2 = lh2 - hh2$	4.3 meV	11.0 meV		
lh3-e3	1.2949	1.3164	0.0215	$7.9 \times 10^{-5}$
hh3-e3	1.2878	1.2998	0.0120	$4.4 \times 10^{-5}$
$\Delta E_3 = lh3 - hh3$	7.0 meV	16.6 meV		

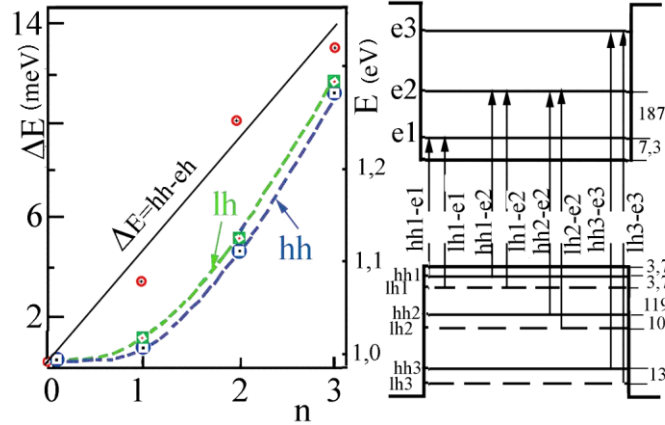


**Fig. 7.** Dependence of energy position of hh, lh bands and the difference  $\Delta E = hh - eh$  on the quantum number  $n$  (left part of the graph), and the scheme of electron transitions and the energy intervals between the energy levels in QWs (right part of the graph).

A change in the crystal temperature as well as in QW structures leads to a change in the crystal lattice parameter. A change in the lattice parameter (at low deformation potentials) leads a change in electronic energy levels which are described by the deformation potential tensor. The change of the level energy at point  $\mathbf{r}$  of the crystal is given by the following expression [20, 21]:

$$\delta E(\mathbf{r}) = \sum_{ij} E_{ij} W_{ij}(\mathbf{r}) \quad (3)$$

where  $W_{ij}(\mathbf{r})$  is the deformation tensor. Uniaxial or biaxial deformation can cause complicated effects due to the change of the crystal symmetry. In the case of uniaxial deformation, the energy of the band edges  $E_c$  and  $E_v$  of a cubic crystal subjected to the deformation  $\Delta$ , can be written in the following form

$$E_i(\Delta) = E_i(0) + E_i(\Delta). \quad (4)$$

At a given temperature and pressure,

$$E_i(T, P) = E_i(T) + E_i \Delta(P), \quad (5)$$

where  $\Delta(P)$  is the deformation caused by the applied pressure  $P$ , and  $E_i(T)$  is the energy of the band edge at normal pressure, which is given by the following expression

$$E_i(T) = E_i(0) + E_{s,i}(T) + E_i \Delta(T). \quad (6)$$

Here  $E_{s,i}$  are the energy levels, and  $\Delta(T)$  is the temperature deformation. One can write further

$$E_i(T, P) = E_i(0) + E_{s,i}(T) + E_i \Delta(T, P). \quad (7)$$

For the energy levels determining the bandgap, we have

$$E_g(T, P) = E_b(0) + [E_{s,c}(T) - E_{s,v}(T)] + (E_{1,c} - E_{1,v}) \Delta(T, P), \quad (8)$$

where  $\Delta(T, P) = \int_0^T \left( \frac{\partial \Delta}{\partial T} \right)_{P_0} dT + \left( \frac{\partial \Delta}{\partial P} \right)_T (P - P_0)$ .

Here the first partial derivative is the temperature coefficient of expansion, and the second partial derivative is the compressibility taken with a negative sign. These macroscopical values have been measured for some semiconductors. From the last equation we have



$$\left(\frac{\partial E_g}{\partial T}\right)_P = \left(\frac{\partial E_{s,c}}{\partial T}\right)_P - \left(\frac{\partial E_{s,v}}{\partial T}\right)_P + [E_{1,c} - E_{1,v}] \left(\frac{\partial \Delta}{\partial T}\right)_P \quad (9)$$

$$\left(\frac{\partial E_g}{\partial P}\right)_T = [E_{1,c} - E_{1,v}] \left(\frac{\partial \Delta}{\partial P}\right)_T \quad (10)$$

Therefore, the temperature coefficient of the energy level shift consists of the electron-phonon and the deformation components. Different temperature coefficients of the QW exciton energy level shift were found from optical transmission spectra of the investigated heterojunctions. This is due to different temperature coefficients of the light and heavy holes bands shift as well as difference of the light and heavy holes effective masses. The energy of the QD transition is 0.9056 and 0.9289 eV at 300 and 30 K, respectively. The temperature coefficient of the QD energy shift  $\beta = \Delta E / \Delta T$  is  $8.3 \times 10^{-5}$  eV/K. This value does not differ from the temperature coefficient of the energy level shift in QW in the limits of the experimental errors ( $\pm 1$  meV). This observation suggests that, in this structure, the shift of the light and heavy holes bands is determined mainly by the temperature component, rather than by the deformation one. There is an ambiguity in the literature concerning the determination of band parameters in the  $\text{In}_y\text{Ga}_{1-y}\text{As}-\text{GaAs}$  system. The published data concerning the conduction band offset at the  $\text{In}_y\text{Ga}_{1-y}\text{As}-\text{GaAs}$  interface  $\Delta E_c / \Delta E_g$  ( $\Delta E_c$  is the difference of the conduction band bottoms of GaAs and  $\text{In}_y\text{Ga}_{1-y}\text{As}$ ,  $\Delta E_g$  is the difference of their bandgaps) are different: 0.52 [22], 0.6 [23], 0.7 [24, 25], 0.83 [26].

The situation with the data about the heavy holes effective mass in GaAs is similar:  $0.62m_0$  [22],  $0.52m_0$  [24],  $0.51m_0$  [26], and  $0.36m_0$  [25] ( $m_0$  is the free electron mass). There is also a discrepancy concerning the dependence of the bandgap  $E_g(y)$  of stressed  $\text{In}_y\text{Ga}_{1-y}\text{As}$  layers in the  $\text{GaAs}-\text{In}_y\text{Ga}_{1-y}\text{As}-\text{GaAs}$  system on the In content ( $y$ ) [23, 28, 29].

In considering the energy spectrum of QW based on the  $\text{GaAs}-\text{In}_y\text{Ga}_{1-y}\text{As}-\text{GaAs}$  system, we used a mean value of  $E_c/E_g = 0.7$  and a linear approximation of the dependence of electron and hole effective masses on the In content ( $y$ ). The electron effective mass of  $\text{In}_x\text{Ga}_{1-x}\text{As}$  solid solutions was determined from the relation  $m^*/m_0 = 0.067 - 0.0603x + 0.0163x^2$ . The effective masses of electrons  $m_e^*$ , heavy  $m_{hh}^*$  and light  $m_{lh}^*$  holes are  $0.050m_0$ ,  $0.312m_0$ , and  $0.074m_0$ , respectively, at  $x = 0.3$ . The bandgap at 300 K was estimated from the relation  $E_g = 1.425 - 1.501x + 0.436x^2$  [30,31], and it was found to be 1.014 eV for an  $\text{In}_x\text{Ga}_{1-x}\text{As}$  layer with  $x=0.3$ . At 10 K, the bandgap was determined from the relation  $E_g = 1.515 - 1.584x + 0.489x^2$ , which is used for the determination of the bandgap at 0 K [30,31]. The bandgap of an  $\text{In}_x\text{Ga}_{1-x}\text{As}$  layer with  $x=0.3$  was determined to be 1.024 eV at 10 K.

The temperature coefficient  $\beta$  of the quantum levels hh2-e2 and hh1-e2 is  $3.2 \times 10^{-5}$  and  $4.6 \times 10^{-5}$  eV/K, respectively. The value of  $\Delta\beta = \beta(\text{hh1-e2}) - \beta(\text{hh2-e2}) = 1.4 \times 10^{-5}$  [eV/K] means that the level hh1 lies below the top of the valence band with an energy separation of 3.7 meV. The energy interval  $E(\text{hh1-e1}) - E_g$  is 0.011 eV. Consequently, taking into account the energy position of the hh1 level, one can deduce that the e1 level is situated 7.3 meV above the conduction band. One can find from the data presented in the table that the energy interval hh1-hh2 is 119 meV, while the interval e1-e2 is 187 meV.

### **3.3 Calculation of the line shape of the QD oscillator, and the 1s state of excitons in QW of an $\text{In}_{0.3}\text{Ga}_{0.7}\text{As}/\text{GaAs}$ structure.**

The excited states with a frequency close to  $\omega_0$  in QWs of semiconductor heterostructures have a mixed exciton-photon nature including both the electromagnetic and the exciton

components [13-15]. These waves in structures with QWs are analogous to exciton polaritons widely investigated in bulk crystals. In the absence of dissipative processes (i.e., at  $\Gamma = 0$ ), the exciton polariton propagates limitless far, supporting continuous coherent transformations from the exciton to the photon and vice-versa. As a result, the dispersion of the hybrid wave is different from the dispersion of non-interacting photons and excitons; that is, a characteristic anti-crossing occurs near the point of the intersection between the initial dispersion branches. The dispersion equation for exciton polaritons in a periodic structure with QWs has been previously deduced [13, 14]. A wave propagating in the direction of the main axis of the structure Z, where the component of the wave vector  $k_{\parallel}$  in the plane of the interface (x,y) is zero and the electric field as well as the dielectric polarization of the medium lay in this plane, was considered. A frequency range  $\Delta\omega$  which is wide as compared to the inverse value of the exciton life time, but narrow as compared to the distance  $|\omega_0 - \omega_0^*|$  from another nearest exciton resonance  $\omega_0^*$  was considered by specifying one of isolated exciton states in the QW (the level e1— hhl(ls), and designating the resonance frequency of the specified exciton as  $\omega_0$  [13-15]. It was shown that an exciton with non-zero two-dimensional wave vector, i.e.,  $K_x = K_y = 0$ , is excited at a normal incidence of the light. The amplitude coefficients of reflection and transmission are determined according to the relations  $r_{QW} = E_r/E_0$ ,  $t_{QW} = E_t/E_0$ . The amplitude coefficient of the reflection from a real four-layered structure “vacuum (0)-coating layer (1)-singular QW (2)-semi-infinite barrier (3)” is related to  $r_{QW}$  according to the following expression:

$$r = r_{01} + \frac{t_{01} t_{10} e^{2i\varphi_1}}{1 - r_{10} r_{QW} e^{2i\varphi_1}} \quad r_{QW} = \frac{r_{01} + r_{QW} e^{2i\varphi_1}}{1 - r_{10} r_{QW} e^{2i\varphi_1}} \quad (11)$$

Here  $r_{ij}$  ( $= -r_{ji}$ ) and  $t_{ij}$  are the amplitude coefficients of reflection and transmission of the light at the incidence from a semi-infinite medium  $i$  ( $i = 0$  in the vacuum,  $i = 1$  in the layer 1) on a semi-infinite medium  $j$ . In equation (12) we have  $\varphi_1 = K(d_1 + a/2)$ , where  $K$  is the polariton wave vector, and  $d_1$  is the thickness of the layer 1. Therefore, the problem of calculation of the reflection spectrum  $R = |r|^2$  is reduced to the determination of the linear response  $r_{QW}(\omega)$ , which is a complex function of the frequency  $\omega$ . The physical meaning of parameters is as follows:  $\tau_0 = (2\Gamma_0)^{-1}$  is the radiative damping of the 2D exciton,  $\omega_0$  is the resonance exciton frequency, and  $\varpi_0$  is its renormalized resonance frequency [13, 14]. These parameters describe the transformation of the complex frequency of the exciton from  $\omega_0 - i\Gamma$  to  $\varpi_0 - i(\Gamma + \Gamma_0)$  induced by the exciton-photon interaction. Previously [13, 14], an analysis has been performed of the reflection and transmission coefficients of heterostructures with QWs, where the reflection  $r_{QW}$  is defined as

$$r_{QW}(\omega) = \frac{i\Gamma_0}{\varpi_0 - \omega - i(\Gamma + \Gamma_0)}; \quad t_{QW}(\omega) = \frac{\varpi_0 - \omega - i\Gamma}{\varpi_0 - \omega - i(\Gamma + \Gamma_0)} \quad (12)$$

$$\omega_0^* = \omega_0 + r_{10} \Gamma_0 \sin 2\varphi, \quad \Gamma_0 = \Gamma_0 (1 + r_{10} \cos 2\varphi). \quad (13)$$

Here  $\omega_0^*$ ,  $\Gamma_0 = (2\tau_0)^{-1}$ ,  $\Gamma = (2\tau)^{-1}$  are the resonance frequency the radiative, and non-radiative exciton damping parameters, respectively, renormalized taking into account the interaction of the exciton with the light wave induced by this exciton and reflected from the external surface. After a number of transformations of the reflection and absorption coefficients, the following expression is obtained for the reflection coefficient [13, 14]:

$$R(\omega) = |r(\omega)|^2 = R_0 + \frac{A+Bx}{1+x^2} \quad (14)$$

where  $X = \frac{\omega - \omega_0^*}{\Gamma}$ ,  $R_0 = r_{01}^2$

$$A = t_{01}t_{10}S[t_{01}t_{10}S - 2r_{01}(1 + S^*)\cos 2\varphi]$$

$$B = 2r_{01}t_{01}t_{10}S\sin 2\varphi, \quad S = \frac{\Gamma_0}{\Gamma}, \quad S^* = \frac{\Gamma_0^*}{\Gamma}$$

According to the Fresnel's formula, at normal incidence of the light on the crystal surface we have:

$$r_{10} = -r_{01} = \frac{n_b - 1}{n_b + 1}, \quad t_{01}t_{10} = \frac{4n_b}{(n_b + 1)^2}. \quad (15)$$

The A and B coefficients can take values of different signs depending on the distance between the center of the QW and the external surface, and, particularly, they can alternately vanish. At  $A = 0$ ,  $B < 0$ , the resonance contour consists of a maximum at  $\omega < \omega_0^*$  and a minimum at  $\omega > \omega_0^*$ . At  $B = 0$ , there is a maximum ( $A > 0$ ) or a minimum ( $A < 0$ ) in the spectrum. According to previous results [13, 14], the best agreement between the calculations and the experimental spectra is obtained at  $\Gamma \approx \Gamma_0$ ,  $\Gamma_0 = (60 \pm 15) \mu\text{eV}$ , which corresponds to the radiative life time of the exciton  $\tau_0 = (2\Gamma_0)^{-1} \approx 2 \times 10^{-12}$  s. The value of  $\hbar\Gamma_0$  lies in the limits of 0.02–0.2 meV for typical structures, for instance,  $\hbar\Gamma_0 = 0.12$  meV in a CdTe/Cd<sub>0.11</sub>Zn<sub>0.87</sub>Te QW with the thickness of 100 Å [12] and  $\hbar\Gamma_0 \approx 27 \mu\text{eV}$  in a In<sub>0.04</sub>Ga<sub>0.96</sub>As/GaAs QW with thickness of 85 Å [13, 14].

In the technological process of producing GaAs–In<sub>y</sub>Ga<sub>1-y</sub>As–GaAs heterojunctions with QWs, QDs are also formed at the interface of heterojunction layers. The technology of producing QW structures is prospective for the elaboration of optoelectronic devices for the infrared spectral range [4-7]. The process of QDs growth in InAs/GaAs heterostructures with a high value of  $d_{\text{eff}}$  thickness was previously investigated [4-12], and it was shown that with increasing the  $d_{\text{eff}}$ , apart from the increase in QD density, the scatter of the QD sizes occurs, and the number of large relaxed clusters of InAs defects increases. This leads to a broadening of the photoluminescence lines of QD and to a decrease in their intensity.

The deepest minimum (strong oscillator) is observed at the energy of 1.0859 eV (Fig. 8) in the reflection and absorption spectra of In<sub>0.3</sub>Ga<sub>0.7</sub>As/GaAs heterojunctions with QWs. This minimum is due to the hh1-e1(1s) transitions. As mentioned above, the bandgap of the In<sub>x</sub>Ga<sub>1-x</sub>As layer with  $x=0.3$  is 1.014 eV. A weaker minimum at the energy of 0.85 eV is due to QDs formed at the interface of heterojunctions. The calculation of the experimental reflection spectra is performed for the 1s states of the hh1-e1 transitions (as a singular oscillator) as well as for two oscillators (one oscillator of QDs and the other oscillator of QWs). A good coincidence of experimental and experimental contours (Fig. 8) is obtained with the following parameters:  $\omega_0(\text{QD}) = 0.985$  eV and  $\omega_0(\text{hh1-e1,1s}) = 1.086$  eV,  $\varepsilon_b = 10.0$ ,  $\omega_{\text{LT}} = 75$  meV, and  $\Gamma = \Gamma + \Gamma_0 = 7.6 \mu\text{eV}$ , where  $\omega_{\text{LT}}$  is the longitudinal-transverse splitting of the polariton in QW, and  $\Gamma$  is the damping parameter. Unfortunately, the value of the effective mass  $M = m_v^* + m_c^*$  was impossible to be determined. The M parameter, as well as the thickness of the deal layer, does not significantly influence the contours of the investigated spectra.

The experimental values of the optical density ( $D = 1 - R - T$ ) were determined from the measured reflection (R) and transmission (T) spectra of the In<sub>0.3</sub> Ga<sub>0.7</sub>As/GaAs quantum structure. The calculations of spectra were also performed taking into account two oscillators of QD and QW (hh1-e1,1s). The calculated and experimental curves of the optical density (Fig. 9) are in satisfactory concordance with the following parameters:  $\omega_0(\text{QD}) = 0.975$  eV and  $\omega_0(\text{hh1-e1,1s}) = 1.076$  eV. The value of  $\varepsilon = \varepsilon_b + \varepsilon_a$  is (10.0+0.07) for the QD oscillator and QW level. The longitudinal-transverse splitting of the polariton in the QW  $\omega_{\text{LT}}$  is 45 meV, and the damping parameter is  $\Gamma_{\text{eff}} = \Gamma + \Gamma_0 = (2.0+40.5) \mu\text{eV}$  for the QD and (1.0+44.5)  $\mu\text{eV}$  for the  $\omega_0(\text{hh1-e1,1s})$  level of the QW. One can see from these data that  $\Gamma_{\text{eff}} \approx \Gamma_0$  and, consequently, the

radiative exciton life time in the QD and in the QW are nearly equal to  $\tau_0 = (2\Gamma)^{-1} \approx 2 \times 10^{-12}$  s.

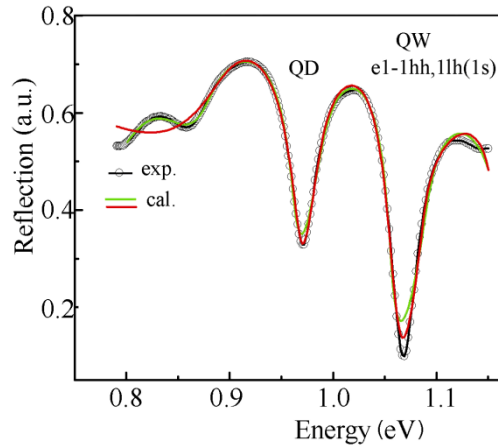


**Fig. 8.** Spectral dependence of the contour of measured (exp.) and calculated (cal.) reflections spectra of an  $\text{In}_{0.3}\text{Ga}_{0.7}\text{As}/\text{GaAs}$  quantum structure.

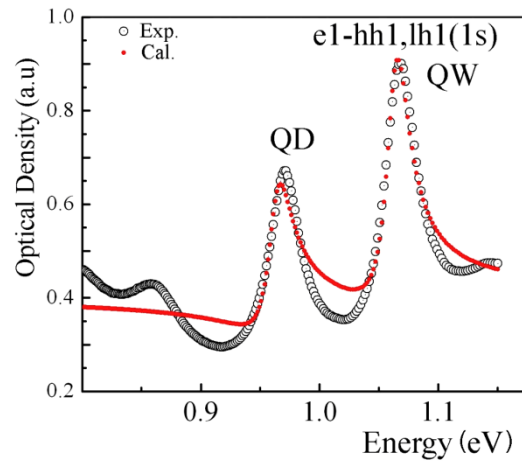


**Fig. 9.** Experimental (Exp.) and calculated (Cal.) optical densities obtained from the measured reflection (R) and transmission (T) spectra as well as from the calculations of an  $\text{In}_{0.3}\text{Ga}_{0.7}\text{As}/\text{GaAs}$  quantum structure.

#### 4. Conclusions

The experimental investigations of  $\text{In}_{0.3}\text{Ga}_{0.7}\text{As}/\text{GaAs}$  heterojunctions with QWs revealed the presence of narrow and intensive lines in optical absorption and reflection spectra which are due to the ground states of exciton polaritons in QWs. Features caused by QDs formed at the interface of nanolayers and the buffer were observed in the optical spectra. The contours of the reflection and transmission lines were calculated both with a single-oscillator, and many-oscillator models. The oscillator strength and the damping parameter of QWs and QDs were estimated from these calculations. These data demonstrate that  $\Gamma_{\text{eff}} \approx \Gamma_0$  and, consequently, the radiative life time of the exciton in the QD and in the QW are nearly equal to  $\tau_0 = (2\Gamma_0)^{-1} \approx 2 \times 10^{-12}$  s.

**Acknowledgments.** Financial support from SCOPES program (project IZ73Z0-128019) is acknowledged.

## References

- [1] N. N. Ledentsov, *Prog. Cryst. Growth*. Ch. 35, 289 (1997).
- [2] L. Goldstein, F. Glas, J.Y. Marzin, M. N. Charasse, and G. Le Roux, *Appl. Phys. Lett.* 47, 1099 (1985).
- [3] P. M. Petroff and S. P. DenBaars. *Superlattice Microst.* 15, 15 (1994).
- [4] N. N. Ledentsov, M. Grundmann, N. Kirstaedter, O. Schmidt, R. Heitz, J. Bohrer, D. Bimberg, V. M. Ustinov, V. A. Shchukin, P. S. Kop'ev, *Zh. I. Alferov*, S. S. Ruvimov, A. O. Kosogov, P. Werner, U. Richter, U. Gosele, and J. Heydenreich, *Solid-State Electron.* 40, 785 (1996).
- [5] N. Kirstaedter, N. N. Ledentsov, M. Grundmann, D. Bimberg, V. M. Ustinov, S. S. Ruvimov, M. V. Maximov, P. S. Kop'ev, *Zh. I. Alferov*, U. Richter, P. Werner, U. Gosele, and J. Heydenreich, *Electron. Lett.* 30, 1416 (1994).
- [6] M. V. Maksimov, N. Yu. Gordeev, S. V. Zaitsev, P. S. Kop'ev, I. V. Kochnev, N. N. Ledentsov, A. V. Lunev, S. S. Ruvimov, A. V. Sakharov, and A. F. Tsatsul'nikov, *Semiconductors* 31, 124 (1997).
- [7] A. R. Kovsh, A. E. Zhukov, D. A. Lifshits, A. Yu. Egorov, V. M. Ustinov, M. V. Maximov, Yu. G. Musikhin, N. N. Ledentsov, P. S. Kop'ev, *Zh. I. Alferov*, and D. Bimberg, *Electron. Lett.* 35, 1161 (1999).
- [8] M. V. Maximov, A. F. Tsatsulinikov, B. V. Volovik, D. A. Bedarev, A. Yu. Egorov, A. E. Zhukov, A. R. Kovsh, N. A. Bert, V. M. Ustinov, P. S. Kopiev, *Zh. I. Alferov*, N. N. Ledentsov, D. Bimberg, I. P. Soshnikov, and P. Werner, in: *Proceedings of the 24th International Conference on the Physics of Semiconductors, ICPS24*, World Scientific, Jerusalem, 1998.
- [9] R. P. Mirin, J. P. Ibbetson, K. Nishi, A. C. Gossard, and J. E. Bowers, *Appl. Phys. Lett.* 67, 3795 (1995).
- [10] D. L. Huffaker, G. Park, Z. Zou, O.B. Shchekin, and D.G. Deppe, *Appl. Phys. Lett.* 73 2564 (1998).
- [11] B. V. Volovik, A. F. Tsatsulinikov, D. A. Bedarev, A. Yu. Egorov, A. E. Zhukov, A. R. Kovsh, N. N. Ledentsov, M. V. Maximov, N. A. Maleev, Yu. G. Musihin, A. A. Suvorova, V. M. Ustinov, P. S. Kopiev, *Zh. I Alferov*, D. Bimberg, and P. Verner, *Semiconductors* 33, 901 (1999).
- [12] N. A. Maleev, A. E. Zhukov, A. R. Kovsh, S. S. Mihin, V. M. Ustinov, D. A. Bedarev, B. V. Volovik, I. L. Krestinov, I. N. Kayander, V. A. Ondobljudov, A. A. Suvorova, A. F. Tsatsulinikov, Yu. M. Shernjakov, N. N. Ledentsov, P. S. Kopiev, *Zh. I. Alferov*, and D. Bimberg, *Semiconductors* 34, 594 (2000).
- [13] E. L. Ivchenko, *Optical Spectroscopy of Semiconductor Nanostructures*, Alpha Science International, Harrow, UK, 2005.
- [14] L. E. Vorobjev, E. L. Ivchenko, D. A. Firsov, and V. A. Shalygin, *Optical Properties of Nanostructures*, in: V.I. Iljin, A.Ja. Shik (Eds.), *Nauka, Sankt-Petersburg*, 2001 (in Russian).
- [15] Mark Fox, *Optical Properties of Solids*, Oxford University Press, 2001.
- [16] L. E. Vorobjev, V. Yu. Panevin, N. K. Fedosov, D. A. Firsov, V. A. Shalygin, S. Hanna, A. Eilmeier, Kh. Moumanis, F. Julien, A. E. Zhukov, and V. M. Ustinov, *Phys. Solid State* 46, 118 (2004).
- [17] L. I. Korovin, I. G. Lang, and S. T. Pavlov, *Phys. Solid State* 48, 2337 (2006).
- [18] I. G. Lang, V. I. Belitsky, and M. Cardona, *Phys. Status Solidi A* 164, 307 (1997).

- [19] L. I. Korovin, I. G. Lang, D. A. Contreras-Solorio, and S. T. Pavlov, *Phys. Solid State* 43, 2182 (2001).
- [20] J. Bardeen and W. Shockley, *Phys. Rev.* 80, 72 (1950).
- [21] E. Johnson, in: *Semiconductors and Semimetals*, Vol. 3, Academic Press, New York and London, 1967.
- [22] I. A. Avrutskii, V. A. Sychugov, and B. A. Usievich, *Fiz. Tekh. Poluprov.* 25, 1787 (1991).
- [23] I. V. Bradley, W. P. Gillin, K. P. Homewood, and R. P. Webb, *J. Appl. Phys.* 73, 1686 (1993).
- [24] G. Ji, D. Huang, U. K. Reddy, T. S. Henderson, R. Houdre, and H. Morkoc, *J. Appl. Phys.* 62, 3366 (1987).
- [25] M. Wojtowicz, D. Pascua, A. C. Han, T. R. Block, and D. C. Streit., *J. Cryst. Growth* 175/176, 930 (1997).
- [26] T. G. Anderson, Z. G. Chen, V. D. Kulakovskii, A. Uddin, and J. T. Valin, *Phys. Rev. B* 37, 4032 (1988).
- [27] L. Pavesi and M. Guzzi, *J. Appl. Phys.* 75, 4779 (1984).
- [28] P. O. Vaccaro, M. Takahashi, K. Fujita, and T. Watanabe, *J. Appl. Phys.* 76, 8037 (1994).
- [29] A. S. Ignatjev, M. V. Karachevtseva, V. G. Makarov, G. Z. Nemtsev, V. A. Strahov, and N. G. Yaremenko, *Fiz. Tekh. Poluprov.* 28, 125 (1994).
- [30] S.L. Chung, *Physics of Optoelectronic Devices*, John Wiley & Sons, New York, 1995.  
J. Menendez, A. Pinczuk, D. J. Werder, S. K. Sputz, R. C. Miller, D. L. Sivko, and A. Y. Cho, *Phys. Rev. B* 36, 8165 (1987).